

Major Differences between the Binuclear Manganese Boronyl Carbonyl $\text{Mn}_2(\text{BO})_2(\text{CO})_9$ and Its Isoelectronic Chromium Carbonyl Analogue $\text{Cr}_2(\text{CO})_{11}$

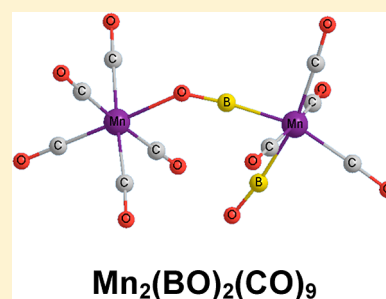
Yu Chang,[†] Qian-Shu Li,^{*,†} Yaoming Xie,[§] and R. Bruce King^{*,†,§}

[†]MOE Key Laboratory of Theoretical Chemistry of Environment, Center for Computational Quantum Chemistry, South China Normal University, Guangzhou 510631, China

[§]Department of Chemistry and Center for Computational Chemistry University of Georgia, Athens, Georgia 30602, United States

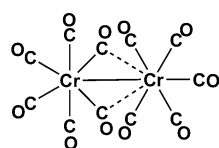
S Supporting Information

ABSTRACT: The lowest energy structures of the manganese boronyl carbonyl $\text{Mn}_2(\text{BO})_2(\text{CO})_9$ by more than 8 kcal/mol are found to have a single end-to-end bridging BO group bonding to one manganese atom through its boron atom and to the other manganese atom through its oxygen atom. The long Mn...Mn distances in these structures indicate the lack of direct manganese–manganese bonding as confirmed by essentially zero Wiberg bond indices. These $\text{Mn}_2(\text{BO})_2(\text{CO})_9$ structures are favored thermochemically by more than 25 kcal/mol over dissociation into mononuclear fragments and thus appear to be viable synthetic objectives. This contrasts with the isoelectronic $\text{Cr}_2(\text{CO})_{11}$ system, which is predicted to be disfavored relative to the mononuclear fragments $\text{Cr}(\text{CO})_6 + \text{Cr}(\text{CO})_5$. Analogous $\text{Mn}_2(\text{BO})_2(\text{CO})_9$ structures with an end-to-end bridging CO group lie ~17 kcal/mol in energy above the corresponding structures with end-to-end bridging BO groups. The lowest energy $\text{Mn}_2(\text{BO})_2(\text{CO})_9$ structures without an end-to-end bridging BO group provide unprecedented examples of the coupling of two terminal BO groups to form a terminal dioxidoborene (B_2O_2) ligand with a B–B distance of ~1.9 Å. Still higher energy $\text{Mn}_2(\text{BO})_2(\text{CO})_9$ structures include singly bridged and doubly semibridged structures analogous to the previously optimized lowest energy $\text{Cr}_2(\text{CO})_{11}$ structures.

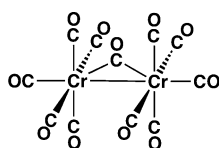


1. INTRODUCTION

The three homoleptic binuclear metal carbonyls $\text{Co}_2(\text{CO})_8$, $\text{Fe}_2(\text{CO})_9$, and $\text{Mn}_2(\text{CO})_{10}$ are stable crystalline solids, which have now been available commercially for a number of years. The next member of this series of binuclear metal carbonyls is the chromium carbonyl $\text{Cr}_2(\text{CO})_{11}$. However, neither this compound nor its molybdenum or tungsten analogues have been isolated. A theoretical study on $\text{Cr}_2(\text{CO})_{11}$ leads to low energy structures having either a single bridging carbonyl group or two semibridging carbonyl groups (Figure 1).¹ Both of these $\text{Cr}_2(\text{CO})_{11}$ structures have Cr–Cr distances consistent with the formal single bonds required to give the chromium atoms the favored 18-electron configurations. However, the dissociation energy of the low-lying $\text{Cr}_2(\text{CO})_{11}$ structure, namely the doubly semibridged structure $\text{Cr}_2(\mu\text{-CO})_2(\text{CO})_9$ (Figure 1) to give $\text{Cr}(\text{CO})_6 + \text{Cr}(\text{CO})_5$ is negative, i.e., –1.7 kcal/mol. This



Doubly semibridged structure



Singly bridged structure

Figure 1. Low energy $\text{Cr}_2(\text{CO})_{11}$ structures found in the previous theoretical study.¹

accounts for the fact that $\text{Cr}_2(\text{CO})_{11}$ has never been synthesized. Any reactions that might be expected to lead to $\text{Cr}_2(\text{CO})_{11}$ instead give the very stable mononuclear $\text{Cr}(\text{CO})_6$.

Simple diatomic ligands related to the carbonyl ligand in these chromium derivatives mentioned above have been of interest for more than a century. Thus, metal complexes of the cyanide (CN),^{2–4} nitrosyl (NO),^{5,6} and carbonyl (CO)⁷ ligands were already known by the end of the 19th century and an extensive coordination chemistry of each of these ligands has developed during the 20th century. In addition, the first metal complex of the dinitrogen ligand, namely $[\text{Ru}(\text{NH}_3)_5\text{N}_2]^{2+}$, was discovered by Allen and Senoff in 1965⁸ and the coordination chemistry of dinitrogen has developed extensively since then.^{9,10} However, metal complexes containing the related diatomic boron ligands BO and BF were synthesized for the first time only very recently owing to synthetic difficulties arising from the instability of the free ligands. Thus only in 2009 the first structurally characterized fluoroborylene (BF) complex, namely, $(\eta^5\text{-C}_5\text{H}_5)_2\text{Ru}_2(\text{CO})_4(\mu\text{-BF})$, was synthesized by Vidović and Aldridge and structurally characterized by X-ray diffraction.¹¹ Even more recently (2010) Braunschweig and co-workers,^{12,13} synthesized the first stable

Received: November 28, 2012

Revised: January 25, 2013

Published: February 12, 2013

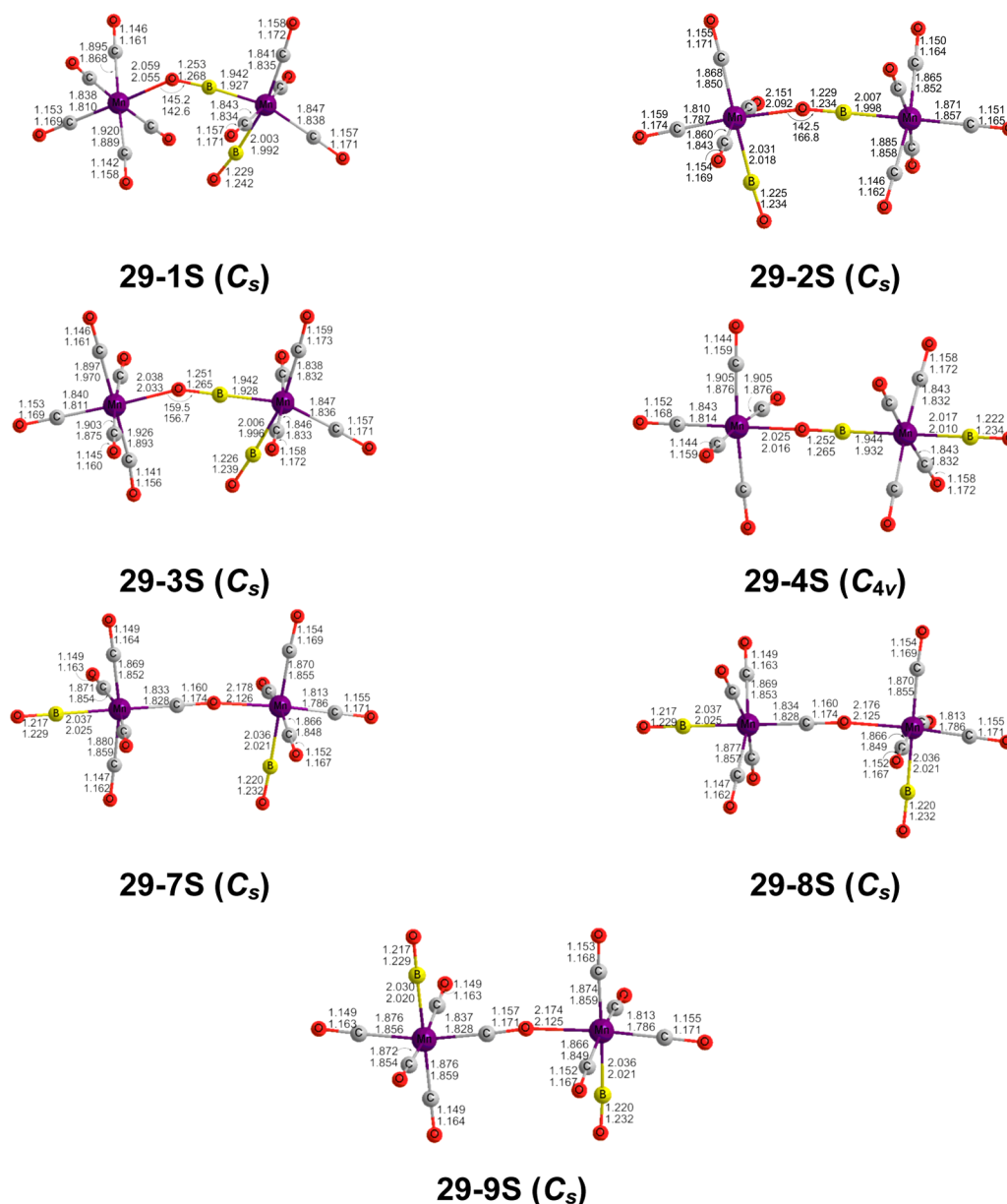


Figure 2. Seven $\text{Mn}_2(\text{BO})_2(\text{CO})_9$ structures with end-to-end bridging BO or CO groups. The bond distances (Å) and bond angles (deg) are from the B3LYP (upper) and BP86 (lower) methods.

boronyl (BO) complex, namely $(\text{Cy}_3\text{P})_2\text{Pt}(\text{BO})\text{Br}$ (Cy = cyclohexyl).

The neutral boronyl ligand (BO) found in this experimentally known platinum complex has one less electron than the carbonyl (CO) ligand and thus functions as a net one-electron donor ligand to a transition metal atom. Alternatively stated, the BO^- anion is isoelectronic with the neutral CO group. Thus $(\text{Cy}_3\text{P})_2\text{Pt}(\text{BO})\text{Br}$ is an example of a planar four-coordinate d^8 metal complex, which is a common feature of platinum(II) chemistry.

Direct boronyl analogues of the homoleptic metal carbonyls remain unknown experimentally but have been investigated theoretically. Thus a theoretical study on cobalt carbonyl boronyls¹⁴ focused on $\text{Co}(\text{BO})(\text{CO})_4$ and $\text{Co}_2(\text{BO})_2(\text{CO})_7$ as isoelectronic analogues of the well-known $\text{Fe}(\text{CO})_5$ and $\text{Fe}_2(\text{CO})_9$, respectively, has been carried out. Similarly, $\text{Fe}_2(\text{BO})_2(\text{CO})_8$ is an isoelectronic analogue of $\text{Mn}_2(\text{CO})_{10}$. A recent theoretical study¹⁵ on $\text{Fe}_2(\text{BO})_2(\text{CO})_8$ predicts an

unbridged structure consisting of two $\text{Fe}(\text{BO})(\text{CO})_4$ units linked by an Fe–Fe bond. A subsequent theoretical study on the unsaturated $\text{Fe}_2(\text{BO})_2(\text{CO})_n$ ($n = 7, 6$) predicts low-energy structures having three-electron donor bridging BO ligands bonded to the iron atoms through not only the boron atom but also the oxygen atom.¹⁶ In addition, higher energy $\text{Fe}_2(\text{B}_2\text{O}_2)(\text{CO})_n$ ($n = 7, 6$) structures were found in which the two BO ligands have coupled through B–B bond formation to form a bridging dioxodiborene (B_2O_2) ligand. An earlier theoretical study by Baerends and co-workers¹⁷ of transition metal complexes comparing the isolobal ligands BF, BNH_2 , $\text{BN}(\text{CH}_3)_2$, and BO predating the discovery of $(\text{Cy}_3\text{P})_2\text{Pt}(\text{BO})\text{Br}$ led to the general conclusion that the BO ligand, considered as a monoanion isoelectronic with CO, is an unusually strong σ donor but a very poor π -acceptor because of the very high energy of its π^* LUMO.

This paper reports a theoretical study on $\text{Mn}_2(\text{BO})_2(\text{CO})_9$, which is isoelectronic with the unknown $\text{Cr}_2(\text{CO})_{11}$. As noted

Table 1. Total Energies (E , Hartree), Relative Energies (ΔE , kcal/mol), Relative Energies Corrected with the Zero Point Vibrational Energy (ΔE_{ZPE} , kcal/mol), and Numbers of Imaginary Vibrational Frequencies (N_{imag}), for the $\text{Mn}_2(\text{BO})_2(\text{CO})_9$ Structures

	BP86				B3LYP			
	E	ΔE	ΔE_{ZPE}	N_{imag}	E	ΔE	ΔE_{ZPE}	N_{imag}
29-1S (C_i)	−3523.13222	0.0	0.0	none	−3522.68799	0.0	0.0	none
29-2S (C_i)	−3523.13062	1.0	1.1	none	−3522.68630	1.1	1.1	none
29-3S (C_i)	−3523.12921	1.9	1.8	1 (15i)	−3522.68528	1.7	1.6	1 (13i)
29-4S (C_{4v})	−3523.11685	9.7	9.5	1 (21i)	−3522.67446	8.5	8.5	none
29-5S (C_{2v})	−3523.11024	13.8	13.5	none	−3522.64479	27.1	26.9	1 (26i)
29-6S (C_i)	−3523.10910	14.5	14.3	none	−3522.64632	26.2	26.0	none
29-7S (C_i)	−3523.10672	16.0	16.0	none	−3522.65975	17.7	17.7	none
29-8S (C_i)	−3523.10670	16.0	16.0	none	−3522.65970	17.8	17.7	none
29-9S (C_i)	−3523.10627	16.3	16.2	none	−3522.65987	17.7	17.6	none
29-10S (C_i)	−3523.10320	18.2	18.0	none	−3522.64198	28.9	28.8	none
29-11S (C_{2v})	−3523.10273	18.5	17.8	2 (134i, 26i)	−3522.65667	19.7	19.1	2 (133i, 26i)
29-12S (C_{2v})	−3523.10236	18.8	18.6	2 (26i, 10i)	−3522.63811	31.3	31.1	1 (26i)
29-13S (C_{2v})	−3523.10065	19.8	19.6	none	−3522.64204	28.9	28.7	none

above, theoretical studies on $\text{Cr}_2(\text{CO})_{11}$ predict the structures depicted in Figure 1 but also predicts such structures to be disfavored with respect to dissociation into mononuclear fragments.¹ In contrast to $\text{Cr}_2(\text{CO})_{11}$, we now predict $\text{Mn}_2(\text{BO})_2(\text{CO})_9$ to be viable with respect to dissociation into analogous mononuclear fragments. Thus $\text{Mn}_2(\text{BO})_2(\text{CO})_9$ appears to be a promising synthetic objective, possibly obtained by the photolysis of $\text{Mn}(\text{BO})(\text{CO})_5$, isoelectronic with the very stable $\text{Cr}(\text{CO})_6$. By analogy with the reported synthesis^{12,13} of $(\text{Cy}_3\text{P})_2\text{Pt}(\text{BO})\text{Br}$, a possible route to this $\text{Mn}(\text{BO})(\text{CO})_5$ precursor to $\text{Mn}_2(\text{BO})_2(\text{CO})_9$ might be the reaction of $\text{NaMn}(\text{CO})_5$ with $\text{Me}_3\text{SiOBBr}_2$ followed by Me_3SiBr elimination from the $\text{Me}_3\text{SiOB}(\text{Br})\text{Mn}(\text{CO})_5$ intermediate.

2. THEORETICAL METHODS

Electron correlation effects were considered by employing density functional theory (DFT), which has evolved as a practical and effective computational tool, especially for organometallic compounds.^{18–24} Two DFT functionals (B3LYP and BP86) were used in this study. These two functionals are constructed in very different ways. B3LYP is a hybrid HF/DFT functional using a combination of the three-parameter Becke functional (B3) with the Lee–Yang–Parr (LYP) generalized gradient correlation functional.^{25,26} It includes exact exchanges and is calibrated by fitting three parameters to a set of experimental results. BP86 combines Becke's 1988 exchange functional (B)²⁷ with Perdew's 1986 gradient corrected correlation functional (P86).²⁸ It does not include exact exchange and is mainly deduced by forcing the functional to satisfy certain exact constraints based on first principles. When these two very different DFT functionals agree, confident predictions can be made. For most of the compounds investigated in this work, both methods agree quite well.

For consistency with our previous research, the same double- ζ plus polarization (DZP) basis sets were adopted in the present study. Thus one set of pure spherical harmonic d functions with orbital exponents $\alpha_d(\text{B}) = 0.7$, $\alpha_d(\text{C}) = 0.75$, and $\alpha_d(\text{O}) = 0.85$ for boron, carbon, and oxygen, respectively, was added to the standard Huzinaga–Dunning contracted DZ sets,^{29,30} designated as (9s5p1d/4s2p1d). The loosely contracted DZP basis set for manganese is the Wachters primitive set,³¹ augmented by two sets of p functions and one set of d

functions, and then contracted following Hood, Pitzer, and Schaefer,³² designated as (14s11p6d/10s8p3d).

The geometries of all structures were fully optimized using the two DFT methods. Harmonic vibrational frequencies were determined by evaluating analytically the second derivatives of the energy with respect to the nuclear coordinates. The corresponding infrared intensities were also evaluated analytically. The $\nu(\text{CO})$ frequencies reported in the present paper were obtained by the BP86 method, which has been shown to give values closer to experimental values without using any scaling factors.^{33,34} This concurrence may be accidental, because the theoretical vibrational frequencies predicted by BP86 are harmonic frequencies, whereas the experimental fundamental frequencies are anharmonic. All of the computations were carried out with the Gaussian03 program package,³⁵ using the fine grid (75, 302) option as the default to evaluate integrals numerically.

A given $\text{Mn}_a(\text{BO})_a(\text{CO})_b$ structure is designated as **ab-cA** where **a** is the number of manganese atoms (the same as the number of BO groups), **b** is the number of CO groups, and **c** orders the structures according to their relative energies. **A** indicates whether the structure is a singlet (**S**) or triplet (**T**). Thus the lowest energy singlet $\text{Mn}_2(\text{BO})_2(\text{CO})_9$ structure is designated **29-1S**.

3. RESULTS

3.1. $\text{Mn}_2(\text{BO})_2(\text{CO})_9$ Structures with an End-to-End Bridging BO or CO Group. Thirteen optimized singlet structures are found for $\text{Mn}_2(\text{BO})_2(\text{CO})_9$ (Figures 2 and 3 and Table 1) within 20 kcal/mol of the global minimum **29-1S**. The lowest energy triplet $\text{Mn}_2(\text{BO})_2(\text{CO})_9$ structure is found to lie at least 30 kcal/mol above the global minimum **29-1S**. Therefore triplet $\text{Mn}_2(\text{BO})_2(\text{CO})_9$ structures are not considered in this paper. The singlet $\text{Mn}_2(\text{BO})_2(\text{CO})_9$ structures include seven structures with end-to-end bridging BO or CO groups without metal–metal bonds, one singly bridged structure with a metal–metal bond, one doubly bridged structure, and four unbridged structures.

The seven end-to-end bridged $\text{Mn}_2(\text{BO})_2(\text{CO})_9$ structures include four BO bridged structures (**29-1S**, **29-2S**, **29-3S**, and **29-4S**) and three CO bridged structures (**29-7S**, **29-8S**, and **29-9S**). All have two octahedrally coordinated Mn atoms bridged by an end-to-end EO ($E = \text{C}$ or B) group bonded to one Mn

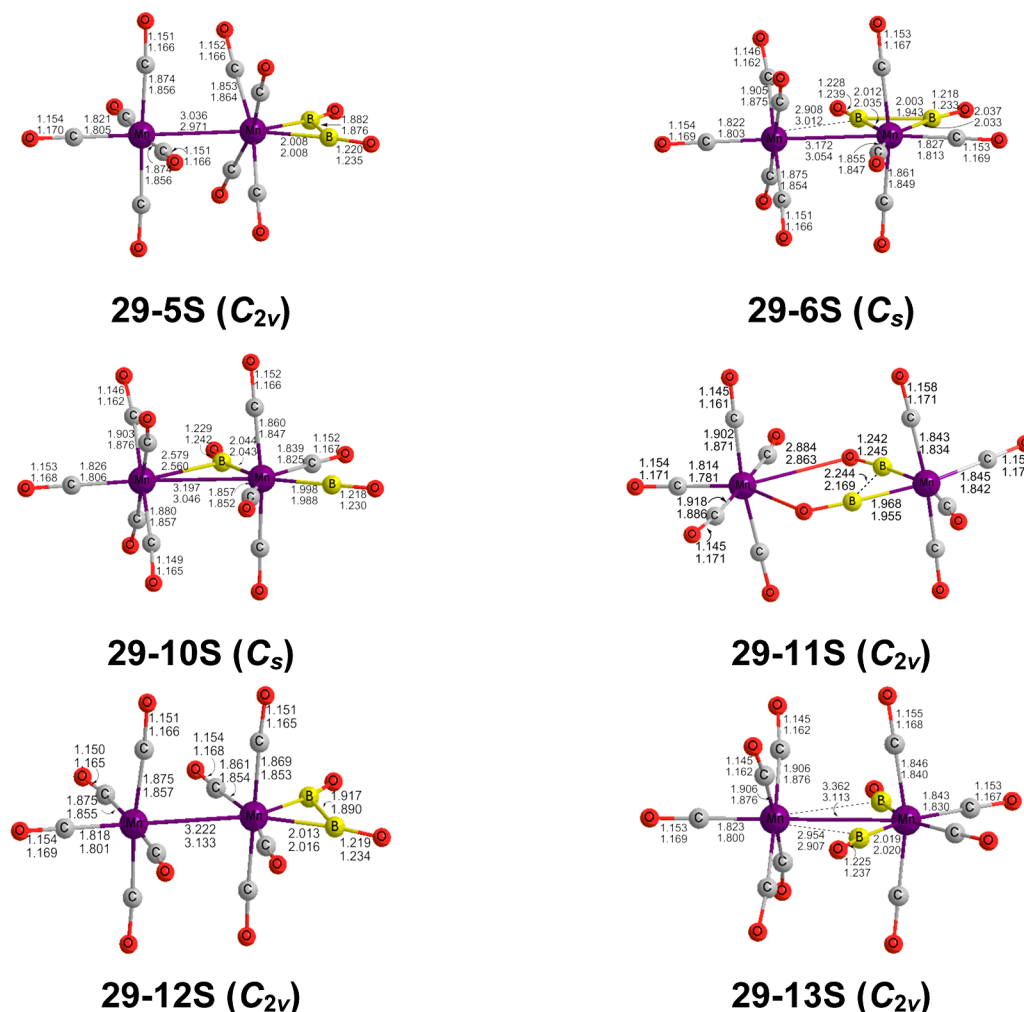


Figure 3. Remaining six $Mn_2(BO)_2(CO)_9$ structures.

atom through the E atom and the other Mn atom through the O atom (Figure 2 and Table 1). The three $Mn_2(BO)_2(CO)_9$ structures with an end-to-end bridging CO group, i.e., **29-7S**, **29-8S**, and **29-9S**, lie ~ 18 kcal/mol (B3LYP) or ~ 16 kcal/mol (BP86) above three of the structures with an end-to-end bridging BO group, i.e., **29-1S**, **29-2S**, and **29-3S** (Table 1).

The three lowest energy $Mn_2(BO)_2(CO)_9$ structures **29-1S** (C_s), **29-2S** (C_s), and **29-3S** (C_s) have one end-to-end BO group bridging an $Mn(CO)_5$ unit to an $Mn(BO)(CO)_4$ unit (Figure 2 and Table 1). They differ in the position of the terminal BO group relative to the central Mn–B–O–Mn bridge. In structures **29-1S** and **29-3S**, the oxygen atom of the end-to-end bridging BO group is bonded to the $Mn(CO)_5$ moiety whereas in **29-2S**, the boron atom of the end-to-end bridging BO group is bonded to the $Mn(CO)_5$ moiety. Structure **29-3S** is a transition state for rotation around the Mn–O bond connecting two **29-1S** minima, one being eclipsed and the other being staggered. The energies of the three structures **29-1S**, **29-2S**, and **29-3S** lie within 2 kcal/mol, suggesting $Mn_2(BO)_2(CO)_9$ to be a potentially fluxional system.

The global minimum $Mn_2(BO)_2(CO)_9$ structure **29-1S** has a bent end-to-end B–O–Mn unit with a predicted $\angle B-O-Mn$ angle of 145.2° (B3LYP) or 142.6° (BP86) (Figure 2 and Table 1). The B–O distance in the end-to-end bridging BO group in **29-1S** is ~ 1.26 Å, which is longer than the typical terminal B–

O distance of ~ 1.23 Å. As a result, the $\nu(BO)$ stretching frequency for the end-to-end BO group is rather low, i.e., 1656 cm^{-1} (BP86), similar to the bridging BO groups in other binuclear boronyl complexes, such as the iron and cobalt carbonyl derivatives $Fe_2(BO)_2(CO)_n$ and $Co_2(BO)_2(CO)_n$.^{14–16}

The $Mn_2(BO)_2(CO)_9$ structure **29-3S** is an eclipsed stereoisomer of **29-1S** with geometric parameters similar to those of **29-1S** (Figure 2 and Table 1). The end-to-end bridging BO group in **29-3S**, like **29-1S**, is predicted to have a bent $\angle Mn-O-B$ angle of 159.5° (B3LYP) or 156.7° (BP86). The B–O distance in the end-to-end bridging BO group of ~ 1.26 Å and the corresponding $\nu(BO)$ stretching frequency of 1679 cm^{-1} (BP86) in **29-3S** are close to those in **29-1S**. Structure **29-3S** lies ~ 1.8 kcal/mol in energy above **29-1S** with a tiny imaginary vibrational frequency of $\sim 15i\text{ cm}^{-1}$ (Table 1). The corresponding normal mode is related to the inner rotation around the Mn–O–B–Mn unit. Following this normal mode leads from the eclipsed structure **29-3S** to the corresponding staggered structure **29-1S**.

The $Mn_2(BO)_2(CO)_9$ structure **29-2S** (C_s) lies 1.1 kcal/mol (B3LYP) or 1.0 kcal/mol (BP86) above the global minimum **29-1S** (Figure 2 and Table 1). The $\angle B-O-Mn$ angle for the end-to-end bridging BO group in **29-2S** of 142.5° (B3LYP) or 166.8° (BP86) is similar to those in **29-1S** and **29-3S**. The B–O distance of ~ 1.23 Å in the end-to-end bridging BO group of

29-2S is much shorter than those in **29-1S** and **29-3S**, but close to the terminal BO distance. The bridging $\nu(\text{BO})$ frequency of 1845 cm^{-1} (Table S38 in the Supporting Information) is in the terminal BO region reflecting the similar BO distances.

The end-to-end bridging BO groups in **29-1S**, **29-2S**, and **29-3S** are all three-electron donors. The Mn...Mn distances of $\sim 5.0\text{ \AA}$ are too long for direct interactions between the two manganese atoms. Thus, the manganese atoms in all three structures have the favored 18-electron configurations. This assumes that the manganese atoms in **29-1S** and **29-3S** are polarized to give zwitterions in which the $\text{Mn}(\text{CO})_5$ manganese has a formal positive charge and the $\text{Mn}(\text{BO})_2(\text{CO})_4$ manganese has a formal negative charge.

The C_{4v} $\text{Mn}_2(\text{BO})_2(\text{CO})_9$ structure **29-4S** has its terminal BO group in a trans position relative to the end-to-end bridging BO group in contrast to structures **29-1S**, **29-2S**, and **29-3S** (Figure 2 and Table 1). Unlike **29-1S**, **29-2S**, and **29-3S**, the Mn–O–B–Mn unit in **29-4S** is linear rather than bent. Structure **29-4S** lies 8.5 kcal/mol (B3LYP) or 9.7 kcal/mol (BP86) above **29-1S**. The B3LYP method predicts **29-4S** to be a genuine minimum. However, the BP86 method predicts **29-4S** to have a small imaginary vibrational frequency of 21 i cm^{-1} . Following the corresponding normal mode leads to a new C_s structure with insignificant changes in geometry and energy ($<0.2\text{ kcal/mol}$). The bridging B–O distance in **29-4S** is predicted to be $\sim 1.26\text{ \AA}$ corresponding to a predicted $\nu(\text{BO})$ frequency of 1685 cm^{-1} (Table S38, Supporting Information).

The $\text{Mn}_2(\text{BO})_2(\text{CO})_9$ structures **29-7S**, **29-8S**, and **29-9S** all have an end-to-end bridging CO group linking two $\text{Mn}(\text{BO})(\text{CO})_4$ units and are predicted to be genuine minima with no imaginary vibrational frequencies (Figure 2 and Table 1). These three structures differ only in the location of the BO groups. This minor geometry difference leads to a close energy spacing of these three structures within 0.3 kcal/mol . Structures **29-7S**, **29-8S**, and **29-9S** are all predicted to lie $\sim 17\text{ kcal/mol}$ in energy above **29-1S**. Structures **29-7S** and **29-9S** are eclipsed structures whereas **29-8S** is a staggered structure. The Mn–O–C–Mn units all three structures (**29-7S**, **29-8S**, and **29-9S**) are slightly bent with $\angle\text{Mn–O–C}$ angles of $\sim 170^\circ$ in contrast to the perfectly linear $\angle\text{Cr–O–C}$ angles for the end-on bridging CO groups in $\text{Cr}_2(\text{CS})_2(\text{CO})_9$ derivatives.³⁶ The C–O distances in the end-to-end bridging carbonyl groups are predicted to be $\sim 1.17\text{ \AA}$, which are slightly longer than the terminal C–O distances. The corresponding $\nu(\text{CO})$ frequencies range from 1975 to 1988 cm^{-1} , which are only slightly below the lowest terminal $\nu(\text{CO})$ frequency (Table S38, Supporting Information). The Mn–O distances to the end-to-end bridging CO groups in **29-7S**, **29-8S**, and **29-9S** are predicted to be $\sim 2.2\text{ \AA}$, which are longer than those in the BO-bridged structures **29-1S**, **29-2S**, and **29-3S**.

3.2. Remaining Six $\text{Mn}_2(\text{BO})_2(\text{CO})_9$ Structures. Five $\text{Mn}_2(\text{BO})_2(\text{CO})_9$ structures containing direct Mn–Mn bonds are found within a 20 kcal/mol energy range (BP86). Four of these structures, namely **29-5S**, **29-6S**, **29-12S**, and **29-13S**, have only terminal CO and BO groups (Figure 3 and Table 1). However, in **29-5S** and **29-6S** the two BO groups have coupled to form a terminal B_2O_2 (dioxodiborene) ligand with B–B distances of $\sim 1.88\text{ \AA}$ for **29-5S** and $\sim 2.0\text{ \AA}$ for **29-6S**. Structure **29-10S** has one bridging BO group. The $\text{Mn}_2(\text{BO})_2(\text{CO})_9$ structure **29-11S** has two bridging BO groups and an Mn...Mn distance clearly too long for a direct metal–metal bond. No CO-bridged $\text{Mn}_2(\text{BO})_2(\text{CO})_9$ structures are found to lie within 30 kcal/mol in energy of **29-1S**.

All four unbridged $\text{Mn}_2(\text{BO})_2(\text{CO})_9$ structures have the two BO groups coordinated to the same manganese atom (Figure 3 and Table 1). They differ mainly in the relative positions of these two terminal BO groups. Three of them, **29-5S**, **29-6S**, and **29-13S**, have staggered arrangements of the four equatorial CO and BO ligands on the two manganese atoms, whereas **29-12S** has an eclipsed arrangement of these ligands (Figure 3). All four of these structures are relatively high-energy structures lying 26 – 31 kcal/mol (B3LYP) or 14 – 20 kcal/mol (BP86) above **29-1S**. Structures **29-6S** and **29-13S** are predicted to be genuine minima. However, structure **29-12S** is a saddle point with one or two small imaginary vibrational frequencies. By following the related normal mode, the eclipsed structure **29-12S** collapses to the staggered structure **29-5S**. Structure **29-5S** is predicted to have a small imaginary vibrational frequency of 26 i cm^{-1} by B3LYP but to be a genuine minimum by BP86. Following the normal mode of the B3LYP imaginary vibrational frequencies reduces the symmetry from C_{2v} to C_2 with little change in geometry and less than 0.6 kcal/mol change in the energy. The Mn–Mn bond distances in the four unbridged $\text{Mn}_2(\text{BO})_2(\text{CO})_9$ structures range from 3.04 to 3.36 \AA (B3LYP) or 2.97 to 3.13 \AA (BP86), suggesting formal single bonds. However, these Mn–Mn single bonds, particularly that in **29-13S**, are somewhat longer than the experimental Mn–Mn single bond in the related $\text{Mn}_2(\text{CO})_{10}$ structure of 2.98 \AA by electron diffraction in the gas phase³⁷ and 2.92 \AA by X-ray crystallography.³⁸ Because each CO group provides two electrons and each BO group provides one electron, the two manganese atoms in all of these unbridged structures have the favorable 18-electron configuration.

The $\text{Mn}_2(\text{BO})_2(\text{CO})_9$ structure **29-10S** is composed of an $\text{Mn}(\text{CO})_5$ unit and an $\text{Mn}(\text{BO})(\text{CO})_4$ unit connected by a semibridging BO group and an Mn–Mn bond, with a staggered configuration of the terminal CO and BO ligands very similar to the lowest energy structure for the isoelectronic $\text{Cr}_2(\text{CO})_{11}$ (Figure 3 and Table 1).¹ Structure **29-10S** lies 28.9 kcal/mol (B3LYP) or 18.2 kcal/mol (BP86) above **29-1S**. The semibridging BO group in **29-10S** has a short Mn–B distance of $\sim 2.04\text{ \AA}$ and a long Mn–B distance of $\sim 2.57\text{ \AA}$ and exhibits a $\nu(\text{BO})$ frequency of 1762 cm^{-1} , which is lower than $\nu(\text{BO})$ frequencies of terminal BO groups (Table S38, Supporting Information). The Mn–Mn distance in **29-10S** of 3.197 \AA (B3LYP) or 3.046 \AA (BP86) is very close to the Cr–Cr single bond distance of 3.148 \AA predicted for the $\text{Cr}_2(\text{CO})_{11}$ global minimum.¹ This suggests a formal single bond in **29-10S**, thereby giving both Mn atoms the favorable 18-electron configuration.

The $\text{Mn}_2(\text{BO})_2(\text{CO})_9$ structure **29-11S** is a relatively high energy structure, lying 19.7 kcal/mol (B3LYP) or 18.5 kcal/mol (BP86) above **29-1S** (Figure 3 and Table 1). Structure **29-11S** has a long Mn...Mn distance of 5.1 \AA , indicating no direct Mn–Mn bonding. The two BO groups in **29-11S** couple to form a bridging B_2O_2 ligand with a relatively long B–B distance of 2.244 \AA (B3LYP) or 2.169 \AA (BP86). This B–B distance is significantly longer than the 1.8 – 2.0 \AA B–B distances predicted for the B_2O_2 ligands in some iron carbonyl structures of the type $\text{Fe}_2(\text{B}_2\text{O}_2)(\text{CO})_n$ ($n = 7, 6$).¹⁶ The B_2O_2 ligand in **29-11S** is bonded to the $\text{Mn}(\text{CO})_4$ manganese through its boron atoms, presumably with an MnB_2 three-center two-electron bond lengthening the B–B distance. The resulting $\text{Mn}(\text{CO})_4(\text{B}_2\text{O}_2)$ unit functions as a bidentate chelating ligand to the $\text{Mn}(\text{CO})_5$ unit through the B_2O_2 oxygen atoms thereby forming an MnB_2O_2 five-membered ring. The B_2O_2 ligand in

29-11S is predicted to exhibit relatively low $\nu(\text{BO})$ frequencies at 1671 and 1722 cm^{-1} (Table S38, Supporting Information). Structure 29-11S has two imaginary vibrational frequencies of 133i and 26i cm^{-1} (B3LYP) or 134i and 26i cm^{-1} (BP86) corresponding to rupture of one of the Mn–O bonds. Therefore, following the corresponding normal modes in 29-11S leads to 29-3S.

3.3. Natural Bond Orbital NBO Analysis. Table 2 lists the Wiberg bond indices (WBI) for the Mn–Mn bonds and the

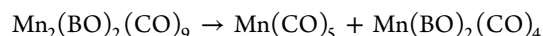
Table 2. Natural Atomic Charges and Wiberg Bond Indices for $\text{Mn}_2(\text{BO})_2(\text{CO})_9$ by the BP86 Method

	natural charge on $\text{Mn}_{\text{left}}/\text{Mn}_{\text{right}}$	Wiberg bond index	Mn–Mn distance (Å)	formal Mn–Mn bond order
29-1S (C_s)	−0.77/−1.23	0.01	4.966	0
29-2S (C_s)	−0.85/−1.15	0.00	5.292	0
29-3S (C_s)	−0.77/−1.23	0.01	5.125	0
29-4S (C_{2v})	−0.77/−1.31	0.01	5.213	0
29-5S (C_{2v})	−0.90/−1.07	0.14	2.971	1
29-6S (C_s)	−0.88/−1.08	0.12	3.054	1
29-7S (C_s)	−1.12/−0.86	0.00	5.118	0
29-8S (C_s)	−1.12/−0.86	0.01	5.120	0
29-9S (C_s)	−1.13/−0.86	0.01	5.119	0
29-10S (C_s)	−0.93/−1.14	0.10	3.046	1
29-11S (C_{2v})	−0.66/−1.21	0.03	5.067	0
29-12S (C_{2v})	−0.86/−1.06	0.15	3.133	1
29-13S (C_{2v})	−0.87/−1.15	0.11	3.113	1

natural charges on the Mn atoms using the BP86 method. The WBIs for metal–metal bonds between transition metals of a given bond order are much lower than those involving main group elements, particularly if the metal–metal bond is bridged by carbonyl groups. For example, the WBI for the triply bridged presumed Fe–Fe bond in $\text{Fe}_2(\text{CO})_9$ is only 0.11.³⁹ Similarly for a hypothetical $\text{Mn}_2\text{S}_2(\text{CO})_8$ structure bridged by a sulfur ligand, the WBIs for the Mn–Mn single bond is predicted to be only 0.14.⁴⁰ This trend continues for the Mn–Mn bonds for the structures discussed in this paper. Thus the Mn–Mn single bonds in the $\text{Mn}_2(\text{BO})_2(\text{CO})_9$ structures 29-5S, 29-6S, 29-10S, 29-12S, and 29-13S all have WBIs ranging from 0.10 to 0.15, similar to that in $\text{Fe}_2(\text{CO})_9$. Furthermore, these WBI values for the formal Mn–Mn single bonds, although relatively low, still differ significantly from the essentially zero (≤ 0.03) WBI values for the long Mn··Mn distances precluding any direct Mn–Mn bonds found in the other $\text{Mn}_2(\text{BO})_2(\text{CO})_9$ structures discussed in this paper.

The natural charge on a Mn atom depends largely on the number of CO and BO groups, especially the number of BO groups (Table 2). Thus an increasing number of Mn–BO bonds from a given manganese atom leads to an increased Mn negative charge. An increasing number of Mn–CO bonds also results in an increased Mn negative charge for a given number of Mn–BO bonds. This suggests that the negative charge on the Mn atom from $\text{OB} \rightarrow \text{Mn}$ or $\text{OC} \rightarrow \text{Mn}$ forward bonding is not completely counterbalanced by the concurrent $\text{Mn} \rightarrow \text{BO}$ or $\text{Mn} \rightarrow \text{CO}$ $\pi \rightarrow \pi^*$ back-bonding. Similar trends have been observed for the natural charges on chromium and iron atoms in their carbonyl derivatives. Thus for the $\text{Mn}_2(\text{BO})_2(\text{CO})_9$ structures, the natural charges on Mn atoms bonded to five carbonyl groups range from −0.66 to −0.93, those on the Mn atoms bonded to four carbonyl groups and one boronyl group range from −0.85 to −0.86, those on the Mn atoms bonded to five carbonyl groups and one boronyl group range from −1.12 to −1.15, and those on the Mn atoms bonded to four carbonyl groups and two boronyl groups range from −1.21 to −1.31.

3.4. Thermochemistry. Dissociation of $\text{Mn}_2(\text{BO})_2(\text{CO})_9$ into mononuclear fragments can lead to formation of either the even-electron species $\text{Mn}(\text{BO})(\text{CO})_5 + \text{Mn}(\text{BO})(\text{CO})_4$ or the odd-electron species $\text{Mn}(\text{CO})_5 + \text{Mn}(\text{BO})_2(\text{CO})_4$ according to the following reactions:



To estimate these dissociation energies, the mononuclear $\text{Mn}(\text{BO})(\text{CO})_5$ and $\text{Mn}(\text{BO})(\text{CO})_4$ structures were optimized using the same DFT methods as were used for the $\text{Mn}_2(\text{BO})_2(\text{CO})_9$ optimizations (Figure 4). Only one singlet $\text{Mn}(\text{BO})(\text{CO})_5$ structure 15-1S was found. Two singlet $\text{Mn}(\text{BO})(\text{CO})_4$ structures 14-1S and 14-2S were found. The $\text{Mn}(\text{BO})(\text{CO})_5$ structure 15-1S is predicted to be a genuine minimum with octahedral manganese coordination. The $\text{Mn}(\text{BO})(\text{CO})_4$ structures can be derived from 15-1S by loss of a carbonyl group either cis to the BO ligand leading to 14-1S or loss of the carbonyl group trans to the manganese atom leading to 14-2S. These $\text{Mn}(\text{BO})(\text{CO})_4$ structures are essentially energetically degenerate with 14-2S, lying only 0.4 kcal/mol (B3LYP) or 1.7 kcal/mol (BP86) above 14-1S.

The dissociation of $\text{Mn}_2(\text{BO})_2(\text{CO})_9$ into mononuclear fragments by either route is predicted to be strongly endothermic, suggesting $\text{Mn}_2(\text{BO})_2(\text{CO})_9$ to be a viable molecule and a reasonable synthetic objective. Thus the

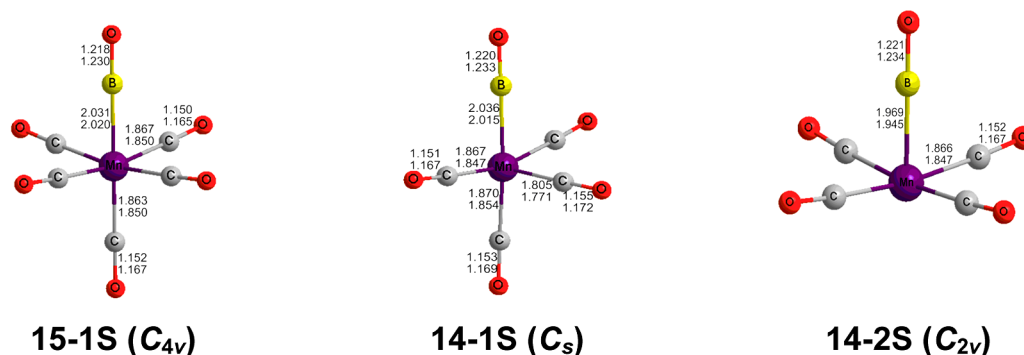


Figure 4. One optimized $\text{Mn}(\text{BO})(\text{CO})_5$ structure and two $\text{Mn}(\text{BO})(\text{CO})_4$ structures.

dissociation energy of $\text{Mn}_2(\text{BO})_2(\text{CO})_9$ to give $\text{Mn}(\text{BO})(\text{CO})_5$ + $\text{Mn}(\text{BO})(\text{CO})_4$ is ~ 27 kcal/mol, and that to $\text{Mn}(\text{CO})_5$ + $\text{Mn}_2(\text{BO})_2(\text{CO})_4$ is ~ 43 kcal/mol (Table 3). Of particular

Table 3. Dissociation Energies (kcal/mol) for the Lowest Energy $\text{Mn}_2(\text{BO})_2(\text{CO})_9$ Structure

	B3LYP	BP86
$\text{Mn}_2(\text{BO})_2(\text{CO})_9 \rightarrow \text{Mn}(\text{BO})(\text{CO})_5 + \text{Mn}(\text{BO})(\text{CO})_4$	27.3	26.2
$\text{Mn}_2(\text{BO})_2(\text{CO})_9 \rightarrow \text{Mn}(\text{CO})_5 + \text{Mn}(\text{BO})_2(\text{CO})_4$	45.8	42.6

interest is that the viability of $\text{Mn}_2(\text{BO})_2(\text{CO})_9$ with respect to such dissociation is quite different from that of the related isoelectronic $\text{Cr}_2(\text{CO})_{11}$, which was predicted to be thermodynamically unfavorable with respect to dissociation into mononuclear fragments.¹

3.5. Vibrational Spectra. In addition to the harmonic vibrational $\nu(\text{CO})$ and $\nu(\text{BO})$ frequencies for $\text{Mn}_2(\text{BO})_2(\text{CO})_9$ in Table S38 (Supporting Information), we also list the $\nu(\text{CO})$ and $\nu(\text{BO})$ frequencies for the optimized mononuclear $\text{Mn}(\text{BO})(\text{CO})_m$ ($m = 5, 4$) in Table 4. All of these $\nu(\text{CO})$

Table 4. Harmonic Vibrational Frequencies $\nu(\text{CO})$ and $\nu(\text{BO})$ (cm^{-1}) for the Mononuclear $\text{Mn}(\text{BO})(\text{CO})_5$ and $\text{Mn}(\text{BO})(\text{CO})_4$ Derivatives Predicted by the BP86 Method (Infrared Intensities (km/mol) in Parentheses)

structures	$\nu(\text{CO})/\text{cm}^{-1}$	$\nu(\text{BO})/\text{cm}^{-1}$
15-1S	2013 (668), 2016 (1279), 2016 (1279), 2036 (0), 2102 (26)	1859 (257)
14-1S	1983 (750), 1993 (1337), 1999 (544), 2070 (73)	1832 (172)
14-2S	1985 (1500), 1985 (1500), 2016 (0), 2079 (7)	1835 (199)
$\text{Fe}(\text{BO})(\text{CO})_4$ (ref 15)	2006 (1216), 2010 (708), 2018 (516), 2075 (96)	1845 (182)
$\text{Co}(\text{BO})(\text{CO})_4$ (ref 14)	2026 (893), 2026 (893), 2039 (471), 2095 (90)	1869 (235)

and $\nu(\text{BO})$ frequencies are predicted by the BP86 method, which has been found to be more reliable than the B3LYP method.^{33,34} These $\nu(\text{CO})$ and $\nu(\text{BO})$ frequencies are all comparable with the corresponding $\nu(\text{CO})$ frequencies for $\text{Fe}(\text{BO})(\text{CO})_m$ and $\text{Fe}_2(\text{BO})_2(\text{CO})_n$ ^{15,16} as well as those for $\text{Co}(\text{BO})(\text{CO})_m$ and $\text{Co}(\text{BO})(\text{CO})_n$.¹⁴

The terminal $\nu(\text{CO})$ frequencies for all of the manganese carbonyl complexes, $\text{Mn}(\text{BO})(\text{CO})_m$ ($m = 5, 4$) and $\text{Mn}_2(\text{BO})_2(\text{CO})_9$, generally range from 1970 to 2124 cm^{-1} , which are lower than that for the free CO molecule⁴¹ owing to the $\text{Mn} \rightarrow \text{CO}$ back-bonding to the π^* antibonding orbital of the CO group. The end-to-end bridging $\nu(\text{CO})$ frequencies in the binuclear manganese boronyl carbonyls are predicted to have only slightly lower frequencies than the terminal carbonyl groups falling in the rather narrow range 1975–1988 cm^{-1} , comparable to the $\nu(\text{CO})$ frequencies of the end-to-end bridging carbonyls in $\text{Cr}_2(\text{CS})_2(\text{CO})_9$.³⁶

The terminal $\nu(\text{BO})$ frequencies in the manganese boronyl carbonyls are predicted to range from 1788 to 1869 cm^{-1} . Similar to terminal $\nu(\text{CO})$ frequencies, these terminal $\nu(\text{BO})$ frequencies lie somewhat below the stretching frequency of 1886 cm^{-1} for the free BO molecule.⁴¹ The $\nu(\text{BO})$ frequency for the semibridging BO group in 29-10S is predicted to be slightly lower at 1763 cm^{-1} . The $\nu(\text{BO})$ frequencies for the chelating BO groups in 29-11S are predicted to lie even lower at 1671 and 1722 cm^{-1} . The end-to-end bridging $\nu(\text{BO})$

frequencies, except for that in 29-2S, range from 1656 to 1685 cm^{-1} and thus are significantly lower than terminal $\nu(\text{BO})$ frequencies. This suggests a lower formal B–O bond order for such end-to-end bridging BO groups.

4. DISCUSSION

The lowest energy $\text{Mn}_2(\text{BO})_2(\text{CO})_9$ structures have a three-electron donor end-to-end bridging BO group bonded to one manganese atom through the boron atom and to the other manganese atom through the oxygen atom. Such structures have long $\text{Mn} \cdots \text{Mn}$ distances, indicating the absence of direct metal–metal bonding as confirmed by Wiberg bond indices of essentially zero. Three structures of this type (29-1S, 29-2S, and 29-3S in Figure 2), differing only in the position of the terminal BO group relative to the $\text{Mn}-\text{B}-\text{O}-\text{Mn}$ bridging unit, lie ~ 8 kcal/mol or more below any of the other ten $\text{Mn}_2(\text{BO})_2(\text{CO})_9$ structures. All three of these structures have the terminal BO group in a cis position relative to the $\text{Mn}-\text{B}-\text{O}-\text{Mn}$ bridging unit. In such structures the $\text{Mn}-\text{B}-\text{O}-\text{Mn}$ unit is bent up to $\sim 142^\circ$. The next higher lying $\text{Mn}_2(\text{BO})_2(\text{CO})_9$ structure 29-4S, lying ~ 9 kcal/mol above 29-1S, also has a similar end-to-end bridging BO group. However, in 29-4S the terminal BO group is in a trans position relative to the $\text{Mn}-\text{B}-\text{O}-\text{Mn}$ bridging unit, which is linear rather than bent.

The stability of these $\text{Mn}_2(\text{BO})_2(\text{CO})_9$ structures with a three-electron donor bridging BO ligand is an indication of the basicity of the oxygen atom of a terminal BO ligand. Thus these structures can be dissected into the mononuclear $\text{Mn}(\text{BO})(\text{CO})_5$ acting as a monodentate oxygen-donor ligand from the boronyl group, which replaces a carbonyl group from a second $\text{Mn}(\text{BO})(\text{CO})_5$ unit. The basicity of the oxygen atom in a terminal BO group has been demonstrated experimentally by the formation of the adducts $(\text{Cy}_3\text{P})_2\text{Pt}(\text{Br})(\text{BO} \rightarrow \text{BR}^f_3)$ (e. g., $\text{R}^f = \text{C}_6\text{H}_3-3,5-(\text{CF}_3)_2$) by reactions of $(\text{Cy}_3\text{P})_2\text{Pt}(\text{BO})\text{Br}$ with boron Lewis acids.⁴²

Our theoretical studies predict a major difference in the viabilities of $\text{Mn}_2(\text{BO})_2(\text{CO})_9$ and the isoelectronic $\text{Cr}_2(\text{CO})_{11}$. Thus whereas $\text{Cr}_2(\text{CO})_{11}$ is predicted¹ to be disfavored with respect to fragmentation into $\text{Cr}(\text{CO})_6 + \text{Cr}(\text{CO})_5$, the isoelectronic $\text{Mn}_2(\text{BO})_2(\text{CO})_9$ is predicted to be viable with respect to analogous fragmentation into $\text{Mn}(\text{BO})(\text{CO})_5 + \text{Mn}(\text{BO})(\text{CO})_4$ by ~ 27 kcal/mol (Table 3). This viability of $\text{Mn}_2(\text{BO})_2(\text{CO})_9$ is undoubtedly a manifestation of the basicity of the oxygen in coordinated BO groups. Also $\text{Mn}_2(\text{BO})_2(\text{CO})_9$ is predicted to be a likely product from the photolysis of the mononuclear $\text{Mn}(\text{BO})(\text{CO})_5$.

The lowest energy $\text{Mn}_2(\text{BO})_2(\text{CO})_9$ structures without bridging BO groups by the B3LYP method, namely 29-5S and 29-6S (Figure 3 and Table 1), have an $\text{Mn}(\text{CO})_5$ unit linked to an $\text{Mn}(\text{B}_2\text{O}_2)(\text{CO})_4$ unit only with an $\text{Mn}-\text{Mn}$ bond analogous to the structure of $\text{Mn}_2(\text{CO})_{10}$. The coupling of two BO groups to form a terminal B_2O_2 ligand linked to the manganese atom through a three-center two-electron MnB_2 bond reduces the effective coordination number of this manganese from seven (with separate BO ligands) to the generally more favorable six (with the MnB_2 three-center bond). The oxygen atoms in these terminal B_2O_2 ligands are located too far from the manganese atom to be involved in the metal–ligand bonding. Thus these terminal neutral B_2O_2 ligands, like two separate BO groups, are effective two-electron donors to the transition metal atom so the coupling of BO groups to form B_2O_2 ligands does not affect the electron

counting. The $\text{Mn}_2(\text{BO})_2(\text{CO})_9$ structures **29-5S** and **29-6S** are the first examples of such terminal B_2O_2 ligands that have arisen in transition metal chemistry, even in theoretically predicted structures. However, bridging B_2O_2 ligands are found in optimized $\text{Fe}_2(\text{B}_2\text{O}_2)(\text{CO})_n$ ($n = 7, 6$) structures, but not the lowest energy ones.¹⁶ The B–B bond distances in the bridging B_2O_2 ligands in these $\text{Fe}_2(\text{B}_2\text{O}_2)(\text{CO})_n$ structures are ~ 1.84 Å. The B–B bond in the terminal B_2O_2 ligand in the $\text{Mn}_2(\text{BO})_2(\text{CO})_9$ structure **29-5S** is only slightly longer at ~ 1.88 Å. The B–B bond in the B_2O_2 ligand in **29-6S** is somewhat longer at ~ 1.97 Å owing to a weak semibridging interaction of one of the boron atoms with the other manganese atom with a long $\text{Mn}\cdots\text{B}$ distance of ~ 3.0 Å.

The three $\text{Mn}_2(\text{BO})_2(\text{CO})_9$ structures **29-7S**, **29-8S**, and **29-9S** were found with single end-to-end bridging CO groups analogous to the end-to-end BO-bridged structures **29-1S**, **29-2S**, and **29-3S**. However, the end-to-end CO-bridged $\text{Mn}_2(\text{BO})_2(\text{CO})_9$ structures lie ~ 17 kcal/mol in energy above the isomeric end-to-end BO-bridged structures. This indicates quite clearly that end-to-end bridging CO groups are less favorable than end-to-end bridging BO groups. The $\text{Mn}_2(\text{BO})_2(\text{CO})_9$ structures **29-7S**, **29-8S**, and **29-9S** with end-to-end bridging CO groups were found to have linear Mn–C–O–Mn units in contrast to the bent Mn–B–O–Mn units of the lowest energy $\text{Mn}_2(\text{BO})_2(\text{CO})_9$ structures **29-1S**, **29-2S**, and **29-3S** with end-to-end bridging BO groups. A similar trend was previously noted in $\text{Cr}_2(\text{CS})_2(\text{CO})_9$ structures with end-to-end bridging CO and CS units in which central Cr–C–S–Cr units are bent but central Cr–C–O–Cr units are linear.³⁶

Structures for $\text{Mn}_2(\text{BO})_2(\text{CO})_9$ were also optimized analogous to the lowest energy predicted $\text{Cr}_2(\text{CO})_{11}$ structures.¹ Thus the singly bridged $\text{Mn}_2(\mu\text{-BO})(\text{BO})(\text{CO})_9$ structure **29-10S** (Figure 3), lying at the relatively high energy of 18–29 kcal/mol above **29-1S** depending on the DFT method, is analogous to the $\text{Cr}_2(\mu\text{-CO})(\text{CO})_{10}$ structure in Figure 1. In addition, the doubly BO-semibridged structure **29-13S** is analogous to the doubly CO-semibridged $\text{Cr}_2(\text{CO})_{11}$ structure in Figure 1. The Mn–Mn distance of 3.113 Å predicted by BP86 for **29-10S** is very close the Cr–Cr distance of 3.148 Å predicted by BP86 for the doubly semibridged structure in Figure 1.¹

5. SUMMARY

The lowest energy $\text{Mn}_2(\text{BO})_2(\text{CO})_9$ structures by more than 8 kcal/mol have a single end-to-end bridging BO group bonding to one manganese atom through its boron atom and to the other manganese atom through its oxygen atom. The long $\text{Mn}\cdots\text{Mn}$ distances in these structures indicate the lack of direct manganese–manganese bonding, as confirmed by essentially zero Wiberg bond indices. These $\text{Mn}_2(\text{BO})_2(\text{CO})_9$ structures are favored thermochemically by more than 25 kcal/mol over dissociation into mononuclear fragments and thus appear to be viable synthetic objectives. This contrasts with the isoelectronic $\text{Cr}_2(\text{CO})_{11}$ system, which is predicted to be disfavored relative to the mononuclear fragments $\text{Cr}(\text{CO})_6 + \text{Cr}(\text{CO})_5$. Analogous $\text{Mn}_2(\text{BO})_2(\text{CO})_9$ structures with an end-to-end bridging CO group lie ~ 17 kcal/mol in energy above the corresponding structures with end-to-end bridging BO groups. This indicates that end-to-end bridging CO groups are less favorable than end-to-end analogous bridging BO groups.

The lowest energy $\text{Mn}_2(\text{BO})_2(\text{CO})_7$ structures without an end-to-end bridging BO group provide unprecedented examples of the coupling of two terminal BO groups to form

a dioxodiborene (B_2O_2) ligand with a B–B distance of ~ 1.9 Å. Still higher energy $\text{Mn}_2(\text{BO})_2(\text{CO})_9$ structures include singly bridged and doubly semibridged structures analogous to the lowest energy $\text{Cr}_2(\text{CO})_{11}$ structures.

■ ASSOCIATED CONTENT

Supporting Information

Table S1: Atomic charges and Wiberg bond indexes for $\text{Mn}_2(\text{BO})_2(\text{CO})_9$ by the B3LYP method. Tables S2–S4: Theoretical Cartesian coordinates (Å) for the $\text{Mn}(\text{BO})(\text{CO})_n$ ($n = 4, 5$) using the B3LYP/DZP and BP86/DZP methods. Tables S5 and S6: Theoretical Cartesian coordinates (Å) for $\text{Mn}(\text{BO})_2(\text{CO})_4$ and $\text{Mn}(\text{CO})_5$ using the B3LYP/DZP and BP86/DZP methods. Tables S7–S19: Theoretical Cartesian coordinates (Å) for the thirteen structures of $\text{Mn}_2(\text{BO})_2(\text{CO})_9$ using the B3LYP/DZP and BP86/DZP methods. Tables S20–S22: Theoretical harmonic vibrational frequencies (cm^{-1}) for $\text{Mn}(\text{BO})(\text{CO})_n$ ($n = 4, 5$) using the B3LYP/DZP and BP86/DZP methods. Tables S23 and S24: Theoretical harmonic vibrational frequencies (cm^{-1}) for $\text{Mn}(\text{BO})_2(\text{CO})_4$ and $\text{Mn}(\text{CO})_5$ using the B3LYP/DZP and BP86/DZP methods. Tables S25–S37: Theoretical harmonic vibrational frequencies (cm^{-1}) for the thirteen structures of $\text{Mn}_2(\text{BO})_2(\text{CO})_9$ using the B3LYP/DZP and BP86/DZP methods. Table S38: Harmonic vibrational frequencies $\nu(\text{CO})$ and $\nu(\text{BO})$ (cm^{-1}) for the binuclear $\text{Mn}_2(\text{BO})_2(\text{CO})_9$ derivatives predicted by the BP86 method. Complete Gaussian 03 reference (ref 35). This information is available free of charge via the Internet at <http://pubs.acs.org>.

■ AUTHOR INFORMATION

Corresponding Author

*E-mail: qslq@scnu.edu.cn (Q.-S.L.); rbking@chem.uga.edu (R.B.K.).

Notes

The authors declare no competing financial interest.

■ ACKNOWLEDGMENTS

We are indebted to the Research Fund for the Doctoral Program of Higher Education (20104407110007), the National Natural Science Foundation of China (Grant 20973066), Guangdong Provincial Natural Science Foundation (S2011010003399) of China, and the U.S. National Science Foundation (Grant CHE-1057466) for support of this research.

■ REFERENCES

- (1) Richardson, N. A.; Xie, Y.; King, R. B.; Schaefer, H. F. *J. Phys. Chem. A* **2001**, *105*, 11134–11143.
- (2) Sharpe, A. G. *Chemistry of Cyano Complexes of the Transition Metals*; Academic: London, 1976.
- (3) Fehlhammer, W. P.; Fritz, M. *Chem. Rev.* **1993**, *93*, 1243–1280.
- (4) Dunbar, K. R.; Heintz, R. A. *Prog. Inorg. Chem.* **1997**, *45*, 283–391.
- (5) Richter-Addo, G. B.; Legzdins, P. *Metal Nitrosyls*; Oxford University Press: New York, 1992.
- (6) Hayton, T. W.; Legzdins, P.; Sharp, W. B. *Chem. Rev.* **2002**, *102*, 935–992.
- (7) Cotton, F. A. *Prog. Inorg. Chem.* **1976**, *21*, 1–28.
- (8) Allen, A. D.; Senoff, C. V. *Chem. Commun.* **1965**, 621–622.
- (9) Henderson, R. A.; Leigh, G. J.; Pickett, C. J. *Adv. Inorg. Chem. Radiochem.* **1983**, *27*, 197–292.
- (10) Sellmann, D.; Sutter, J. *Acc. Chem. Res.* **1997**, *3*, 460–469.
- (11) Vidović, D.; Aldridge, S. *Angew. Chem., Int. Ed.* **2009**, *48*, 3669–3672.

- (12) Braunschweig, H.; Radacki, K.; Schneider, A. *Science* **2010**, *328*, 345.
- (13) Braunschweig, H.; Radacki, K.; Schneider, A. *Angew. Chem., Int. Ed.* **2010**, *49*, 5993–5996.
- (14) Gong, X.; Li, Q.-S.; Xie, Y.; King, R. B.; Schaefer, H. F. *Inorg. Chem.* **2010**, *49*, 10820–10832.
- (15) Chang, Y.; Li, Q.-S.; Xie, Y.; King, R. B.; Schaefer, H. F. *New J. Chem.* **2012**, *36*, 1022–1030.
- (16) Chang, Y.; Li, Q.-s.; Xie, Y.; King, R. B. *Inorg. Chem.* **2012**, *51*, 8904–8915.
- (17) Ehlers, A. W.; Baerends, E. J.; Bickelhaupt, F. M.; Radius, U. *Chem.—Eur. J.* **1998**, *4*, 210–221.
- (18) Ziegler, T.; Autschbach, J. *Chem. Rev.* **2005**, *105*, 2695–2722.
- (19) Bühl, M.; Kabrede, H. *J. Chem. Theory Comput.* **2006**, *2*, 1282–1290.
- (20) Brynda, M.; Gagliardi, L.; Widmark, P. O.; Power, P. P.; Roos, B. O. *Angew. Chem., Int. Ed.* **2006**, *45*, 3804–3807.
- (21) Sieffert, N.; Bühl, M. *J. Am. Chem. Soc.* **2010**, *132*, 8056–8070.
- (22) Schyman, P.; Lai, W.; Chen, H.; Wang, Y.; Shaik, S. *J. Am. Chem. Soc.* **2011**, *133*, 7977–7984.
- (23) Adams, R. D.; Pearl, W. C.; Wong, Y. O.; Zhang, Q.; Hall, M. B.; Walensky, J. R. *J. Am. Chem. Soc.* **2011**, *133*, 12994–12997.
- (24) Lonsdale, R.; Olah, J.; Mulholland, A. J.; Harvey, J. *An. J. Am. Chem. Soc.* **2011**, *133*, 15464–15474.
- (25) Becke, A. D. *J. Chem. Phys.* **1993**, *98*, 5648–5652.
- (26) Lee, C.; Yang, W.; Parr, R. G. *Phys. Rev. B* **1988**, *37*, 785–789.
- (27) Becke, A. D. *Phys. Rev. A* **1988**, *38*, 3098–3100.
- (28) Perdew, J. P. *Phys. Rev. B* **1986**, *33*, 8822–8824.
- (29) Dunning, T. H. *J. Chem. Phys.* **1970**, *53*, 2823–2833.
- (30) Huzinaga, S. *J. Chem. Phys.* **1965**, *42*, 1293–1302.
- (31) Wachters, A. J. H. *J. Chem. Phys.* **1970**, *52*, 1033–1036.
- (32) Hood, D. M.; Pitzer, R. M.; Schaefer, H. F. *J. Chem. Phys.* **1979**, *71*, 705–712.
- (33) Jonas, V.; Thiel, W. *J. Chem. Phys.* **1995**, *102*, 8474–8484.
- (34) Silaghi-Dumitrescu, I.; Bitterwolf, T. E.; King, R. B. *J. Am. Chem. Soc.* **2006**, *128*, 5342–5343.
- (35) Frisch, M. J.; et al. *Gaussian 03*, Revision D 01; Gaussian, Inc.: Wallingford, CT, 2004 (see Supporting Information for complete reference).
- (36) Zhang, Z.; Li, Q.-S.; Xie, Y.; King, R. B.; Schaefer, H. F. *J. Phys. Chem. A* **2010**, *114*, 486–497.
- (37) Almenningsen, A.; Jacobsen, G. G.; Seip, H. M. *Acta Chem. Scand.* **1969**, *23*, 685–686.
- (38) Martin, M.; Rees, B.; Mitschler, A. *Acta Crystallogr.* **1963**, *B38*, 6–15.
- (39) Wang, H.; Xie, Y.; King, R. B.; Schaefer, H. F. *J. Am. Chem. Soc.* **2006**, *128*, 11376–11384.
- (40) Dou, N.; Peng, B.; Li, Q.-s.; Xie, Y.; King, R. B.; Schaefer, H. F. *Polyhedron* **2012**, <http://dx.doi.org/10.1016/j.poly.2012.05.023>.
- (41) Huber, K. P.; Herzberg, G. *Molecular Spectra and Molecular Structure IV. Constants of Diatomic Molecules*; Van Nostrand: New York, 1979.
- (42) Braunschweig, H.; Radacki, K.; Schneider, A. *Chem. Commun.* **2010**, *46*, 6473–6475.